The photoelectron angular distribution of water clusters

Chaofan Zhang,[1] Tomas Andersson,[1] Marko Förstel,[2] Melanie Mucke,[2,a] Tiberiu Arion,[2,b] Maxim Tchaplyguine,[3] Olle Björneholm,[1] and Uwe Hergenhahn[4,c]

[1]*Department of Physics and Astronomy, Uppsala University, Box 516, 751 20 Uppsala, Sweden*

[2]*Max-Planck-Institut für Plasmaphysik, EURATOM Association, Boltzmannstr. 2, 85748 Garching, Germany*

[3]*MAX-lab, Lund University, Box 118, 22100 Lund, Sweden*

[4] *Max-Planck-Institut für Plasmaphysik, EURATOM Association, Wendelsteinstr. 1, 17491 Greifswald, Germany*

The angular distribution of photoelectrons emitted from water clusters has been measured by linearly polarized synchrotron radiation of 40 and 60 eV photon energy. Results are given for the three outermost valence orbitals. The emission patterns are found more isotropic than for isolated molecules. While a simple scattering model is able to explain most of the deviation from molecular behavior, some of our data suggest also an intrinsic change of the angular distribution parameter. The angular distribution function was mapped by rotating the axis of linear polarization of the synchrotron radiation.

---

[a] Present address: Department of Physics and Astronomy, Uppsala University, Box 516, 751 20 Uppsala, Sweden.

[b] Present address: Institut für Experimentalphysik, Universität Hamburg, Luruper Chaussee 149, 22761 Hamburg, Germany.

[c] Corresponding author. Mail address: IPP, c/o Helmholtz-Zentrum Berlin, Albert-Einstein-Str. 15, 12489 Berlin, Germany; electronic address: uwe.hergenhahn@ipp.mpg.de

I. INTRODUCTION

The key to improving understanding of the behavior of liquid water is to comprehend the details of hydrogen bonding. The quest for unraveling these details has motivated a growing interest in the valence electronic structure of water molecules,[1,2] liquid,[3,4] ice[4] and clusters.[5,6] In these works, the binding energies of valence electrons were studied by photoelectron spectroscopy (PES). In water molecules, three orbitals, designated as $1b_1$, $3a_1$ and $1b_2$, make up the outer valence shell. While $1b_1$ is a non-bonding orbital of oxygen lone pair character, the other two orbitals are bonding. Going from molecules to any of the condensed phases, the following changes are observed in the photoelectron spectra: 1. All sharp vibrational peaks are washed out, the spectrum broadens and features of the three different orbitals start to blend in energy. This observation has been well reproduced by suitable sampling of the initial state energies over the space accessible to the isomers of the water ensemble.[6] 2. The $1b_1$ orbital loses its non-bonding character.[7] Of the three valence orbitals, this one broadens the most, and develops into a new feature at substantially lower binding energy, which is characteristic for water condensation observed in PES.[5,6] 3. Besides this, all binding energies shift to lower values due to final state polarization.[3,6] An alternative experimental method to study the valence electronic structure is X-ray emission spectroscopy.[8]

From gas phase PES it is well known that photoelectrons are emitted anisotropically whenever the ionizing radiation makes out a distinct spatial direction.[9] While this effect is general, we here focus on fully linearly polarized synchrotron radiation as the ionization source. The photoelectron angular distribution (PAD) then shows a directional propensity with respect to the polarization axis. If interaction between the sample and the electric field of the radiation is taken into account up to the dipole order (the usual approximation), and if the sample itself is unordered and non-chiral, all information on the PAD is contained in a single

parameter β (see below). For isolated atoms and molecules, preferential emission of the photoelectrons along the polarization axis, expressed by positive values of β, is the common case. The exact value of β depends on the intrinsic response of the ionized orbital to the applied field, and (for molecules) on scattering effects which the continuum electron experiences in the potential of the ionized molecule. This is why, in principle, PADs contain information both on geometry and electronic structure of the probed sample. As this information is condensed into a single parameter, theory is often needed to allow for definite conclusions.

In case of clusters, in addition to the two factors mentioned above, effects of the aggregation on the angular distribution have to be taken into account. Elastic final state scattering on other atoms or molecules within the cluster will produce a more isotropic angular distribution, i.e. the absolute value of β shifts towards zero compared to the molecular case. It is, however, less clear how initial state effects affect the β parameter. The cluster sizes we probe here (see below) are smaller than the onset of crystallization in water clusters.[10] We therefore assume that solid state band structure effects, e.g. band dispersion, do not play a role in our sample. It seems nevertheless plausible that aggregation will have some influence on the β parameter. Guided by theoretical studies of water orbital shapes in small clusters,[6,7] we expect that the *p* character of the orbitals will change. In water molecules, the orbital with the least amount of *p* character, the $1b_2$, has the least anisotropic photoemission pattern among the outer valence orbitals. For the other two outer valence orbitals, we expect that any hydrogen bonding between water molecules will lead to a lowering of its oxygen p character and hence to a lower photoemission anisotropy and a lower value of β.

The PAD of isolated water molecules has been reported by Truesdale *et al*.[11] and Banna *et al*.[2] already in the 1980s. For water clusters, no previous work on the PAD is known

to us. In a pioneering work on the photoelectron spectrum of liquid water, the authors were using β values taken from molecular water in part of their analysis.[3] PADs have been studied for rare gas clusters though.[12–17] These studies compared the PAD of several rare gas core and valence photoelectron lines to the ones for atomic photoemission. For photoelectron lines with a strongly anisotropic atomic emission pattern and a kinetic energy below approx. 40 eV, a significant reduction of β was observed in the cluster case. The reduction did only weakly depend on the orbital looked at (Xe 5p,[13] Kr 4p,[14] Ar 3s,[15] Ar 3p[17], Xe-Kr-Ar comparison[16]). The authors concluded that variations of β between atoms and atomic clusters are caused by final state elastic scattering of the outgoing photoelectron, and that orbital-specific effects such as band formation do not play a role for the decrease of β.[15] We would like to make two remarks about these results: 1. It is believed that the authors refer to *intra*cluster scattering. *Inter*cluster scattering could also be considered as the cause of such β deviations, but usually has a smaller probability due to the dilute nature of the cluster beam. 2. Meanwhile, at even lower photon energy than studied in those works, evidence for band formation in Ar clusters from the shape of valence photoelectron spectra has been presented.[18]

β measurements of the rare gas clusters at higher kinetic energies are less straightforward in their interpretation. They should be affected much less by intracluster elastic scattering, as the respective cross sections have pronounced maxima at kinetic energies around 10 eV and drop by factors between 3 and 6 for an electron energy of 100 eV.[19] Consequentially, for the Xe 4d line of $\langle N \rangle$ = 270 clusters Rolles *et al*. found identical β values between atoms and clusters, even in an energy range with a pronounced photoelectron anisotropy (photon energies 135-150 eV, kinetic energies 85-100 eV).[13] On the other hand, the same authors found significantly lowered β values for Ar 3s of similar size Ar clusters at kinetic energies up to 70 eV.[15] Öhrwall *et al*. measured the Xe 4d cluster surface/bulk

intensity ratio under two different emission angles for large Xe clusters ($\langle N \rangle$ = 4000), and also found evidence for a significant reduction of β for the bulk contribution.[12]

In the present work, the PAD of valence states of water clusters was experimentally studied. Photon energies of 40 and 60 eV were chosen to explore effects from photoelectron scattering, which apparently depend on kinetic energy. Unlike in rare gas clusters, the spectral features from uncondensed water monomers and from clusters overlap in energy. We have therefore partitioned the measured β parameters to isolate the photoemission from clusters. Our results are compared with a simple model calculation on the effect of elastic scattering.

II. EXPERIMENTAL

In the present study, the PAD anisotropy parameters of both water gas vapor and water clusters have been derived from photoelectron spectra measured with linearly polarized synchrotron radiation.

Water clusters were produced by supersonic expansion of water vapor through a conical nozzle. Water vapor was generated by heating of a water container mounted inside the expansion chamber. A copper nozzle of 80 µm diameter, with a half-opening angle of 15°, and a length of 1100 µm was used. A skimmer was mounted between the expansion chamber and the ionization chamber, in which the water cluster interacted with the synchrotron radiation. More details of the setup have been published elsewhere.[6,20] The measurements in this study were carried out at the UE 112 / PGM 1 beamline at the synchrotron radiation source BESSY II, part of the Helmholtz-Zentrum Berlin, Germany. Photoelectrons emitted from the cluster beam as the result of ionization were collected by a commercial hemispherical electron analyzer (Scienta ES 200). The spectrometer was mounted at the

magic angle of 54.7° with respect to the horizontal and in the plane perpendicular to the photon propagation direction (dipole plane).

One data set was recorded for a photon energy of 40 eV, and one for 60 eV. For the 60 eV data set, seeding of the water jet with He was used. Values of a second 60 eV data set recorded without seeding gas, but of statistically lower quality and subject to larger pressure variations, are also shown.

In order to study the PAD of the sample, the spectrometer has to collect the electrons at different angles with respect to the vector of the linearly polarized radiation. In this work, instead of using multiple spectrometers or a rotatable spectrometer, like in Ref.s [9,11,12–17], the polarization axis of the linearly polarized radiation has been rotated by utilizing the undulator. The principle of the (Apple II) undulator as such has been described elsewhere.[21,22] Applying this method of rotating the light polarization to measuring the PAD is relatively novel. To the best of our knowledge, the only measurement of β by rotating the linear polarization vector is by Godehusen *et al.*[23]

The photoelectron spectra of gas-phase water and water clusters were measured at several different polarization angles. In the photoelectron spectra of the water clusters, coexisting in the beam with free water molecules, the contributions of different cluster and molecular valence orbitals are partly overlapping. The pass energy of the hemispherical analyzer was set to 20 eV. The instrumental broadening of the spectra is estimated to be approximately 50-80 meV, in good agreement with the width of the photoelectron peak of the water-monomer $^1b_1$ orbital. Spectra have been calibrated using the binding energy of the $^1b_1$ orbital of the gas-phase water component, namely 12.61eV (Ref. [1]). Nominal photon energies at this beamline are supposed to be correct within better than 10 meV, therefore no further correction or calibration has been attempted.

Raw data were normalized for variation of the beam current. Variations of the number density of clusters in the interaction region, due to small drifts in the cluster source operation parameters, were estimated from the cluster photoline intensities in reference spectra recorded repeatedly. Where appreciable, we corrected for such drifts. In the resulting spectra, peak areas were determined by integrating the traces between suitable upper and lower energy values. A linear background was subtracted. For the photoelectron line of the $1b_1$ orbital, the separation into monomer and cluster contributions in the spectra is obvious, because the monomer lines consist of only a few sharp vibrational peaks.[1] In this case, the putative $1b_1$ contributions in the spectrum were separated into a cluster contribution with binding energy lower than the adiabatic ionization potential of water monomers, a monomer component, and a cluster component overlapping with the monomer lines. The energetically separated cluster component will be designated as 'HOMO' in the remainder of the text.

The resulting areas were fitted to the analytical form of the differential cross section for photoelectrons excited by partially linearly polarized light, and collected within the dipole plane:[24]

$$\frac{d\sigma}{d\Omega} = \frac{\sigma}{4\pi}\left[1+\frac{\beta}{4}\left(1+3P\cos 2(\theta-\lambda)\right)\right]. \qquad (1)$$

Here, β is the anisotropy parameter, σ is the total photoionization cross section, θ is the angle between the horizontal and the photoelectron emission direction (within the dipole plane), λ is the angle of the major axis of the polarization ellipse to the horizontal, and P is the degree of linear polarization. In our set-up, θ amounts to the 'magic angle' of 54.7°; λ was varied by changing the undulator field. Experimentally, the β parameter for each specific orbital can be determined from the measured angular dependence of the signal. β is bounded between –1 and 2. A higher β means a larger differential cross section in the direction parallel to the

polarization vector of the radiation. In other words, the emission of electrons is more anisotropic. $\beta = 0$ corresponds to isotropic emission.

While for the $1b_1$ orbital contributions of clusters and monomers could be separated spectroscopically, this was not possible for the other two orbitals. We have nevertheless attempted to arrive at cluster-specific β values by partitioning the value determined from the overlapping monomer and cluster contributions. The cluster contribution for the respective feature will be denoted by *c*, defined as the cluster area divided by total area. *c* was determined for the $1b_1$ photoelectron line, and it was assumed that it has the same value for the $3a_1$ and $1b_2$ orbitals. Using this value, and the gas phase reference β from Tab. I, we have partitioned the measured β according to $\beta = c\beta_{cl} + (1 - c)\beta_m$, where subscripts cl and m distinguish the cluster and monomer components. Further details are given below.

In our data analysis, we have inserted fixed values of $P = 1$ and $\lambda = 0$, and have extracted values for σ and β from the least squares fit of eq. (1) to the peak areas. As the values for σ cannot be normalized to an absolute scale, only the results for β will be discussed.

Due to limited time available for this study, we were not able to perform a systematic calibration of the polarization properties of the beamline. Some information on the performance of the undulator in the rotatable linear polarization mode comes from an earlier polarimetry study.[25] Using the BESSY polarimeter the very high degree of polarization for horizontal linear setting was confirmed. The main depolarizing effect was interconversion between S_2 and S_3 polarization components (with these two components of the Stokes vector **S** describing the degree of 45° linear polarization, and the degree of circular polarization). Effectively this leads to a slight variation of the degree of linear polarization *P* with the angle of the measurement: While $P > 0.98$ for horizontal polarization, it could be as low as 0.94 for

45° linear polarization. In our study, in some of our data sets we see systematic deviations of the intensity observed under some angles from the least squares fit. This effect however fails to reproduce for other data sets of a comparable quality. We concluded that fluctuations of our intensity data due to factors outside of the beamline properties, most notably density fluctuations of the cluster target and imperfections in peak-background separation in the spectra, are as important as any hypothetical systematic depolarization effect outlined above. Repeating our angle dependent fits with $P = 0.98$ leads to an increase of the resulting β parameters of less than 3 %.

Error bars for the β values were determined as follows: For a representative data set, the fit of the peak areas was repeated, but arbitrarily assigning a relative error of 10 % to every peak area. This is assumed to be an upper limit for the combined inaccuracies of area determination due to peak-background separation, angle dependent intensity changes of the undulator radiation, incompletely corrected pressure variations, etc. Statistical errors are minor with respect to the above factors. The error of β yielded as output of the fit program thus was 0.1 for $\beta = 0.8$ and 0.06 for $\beta = 1.5$. These figures were used as error bars for all β values below and above unity, respectively. For the second 60 eV data set, they were slightly enlarged, as target pressure fluctuations were larger for this data set. The possible influence of depolarization on our results (< 3 %, see above) is not included in the quoted error bars. In a second part of the analysis, the influence of the monomer fraction was approximately removed from the data, as explained below in further detail.

As mass spectroscopy was not available to us in this set-up, the size of the clusters was determined by using a scaling law.[6,26,27] We obtained mean cluster sizes of $\langle N \rangle = 58$ for the 40 eV data set, and $\langle N \rangle = 84$ for both 60 eV data set (more details are available in the Ref. [28]). For the 40 eV data set, the nozzle temperature had to be estimated from the heating power,

instead of a thermocouple reading. We therefore indicate a larger uncertainty of the mean cluster size. The actual mean cluster size of the first 60 eV data set could be larger, as the use of seeding gas usually improves clusterization but is not taken into account in the scaling parameter formalism. The alternative approach of determining the cluster size from the energy shift of the HOMO peak with respect to the monomer line, as suggested by some of the authors,[6] leads to much lower mean cluster sizes: 37 for the 40 eV data, 30 for the first 60 eV data set (seeded expansion), and 16 for the second 60 eV data set. On the one hand, this confirms our assumption that the seeded water expansion results in a larger cluster size. On the other hand, different than in Ref. [6], values are in a large discrepancy to the scaling law data, and even suggest a size ordering which is reverse to the scaling law. This suggests, that the centroid position of the HOMO peak for a given cluster size is photon energy dependent, a point which had not been discussed in Ref. [6]. All experiments described in Ref. [6] had been done at hν = 30 eV. Below, we will refer to the mean cluster size of the first 60 eV data set as $\langle N \rangle \geq 84$.

III. RESULTS

As the first step of the study, the PAD parameters of gas-phase water monomers were derived from the experiment (see Fig.3 in Ref. [28]) and compared to published results (see Table I). The gas phase monomers were produced by lowering the stagnation pressure of the reservoir and the nozzle temperature until no spectral lines with lower binding energies than the gas phase adiabatic $1b_1$ peak were seen. The β parameters measured by us agree with the literature data within the respective error bars. For 60 eV photons, our data points show a trend towards a slightly larger β than in earlier experiments (see below). All three orbitals treated in our study are predominantly of O 2*p* character. The inner valence ($2a_1$) orbital, of mostly O 2*s* character, was not recorded. The $1b_1$ and $3a_1$ orbitals consistently have a more

anisotropic angular distribution than the $1b_2$ orbital. This has been explained by the lone pair character of the two former orbitals, while the $1b_2$ is strongly involved in intermolecular hydrogen bonding.[29] Also the (in-plane) $3a_1$ orbital has a bonding character, which lowers its β value somewhat compared to the $1b_1$. Calculated β values of the latter are practically identical to calculated ones of the atomic O $2p$ orbital.[30] It is interesting that these values exceed those of the $2p$ orbital in (isoelectronic) Ne, a fact which according to our knowledge has not been explained.

With the reliability of our procedure established, we now turn to a discussion of the results for clusters (Figure 1). Figure 2 shows two typical spectra from our measurements, containing overlapping contributions from the water monomers and from clusters. Similar spectra, but for larger water clusters, were recorded by Öhrwall *et al*.[31] and by others.[5,6] In order to extract the β parameters, we have separated the spectra into four separate regions (I-IV). While the least strongly bound region I contains signal from cluster photoemission only, in all remaining regions the signal of clusters is blended with those of monomers. In region II, the few sharp vibrational lines of the $1b_1$ monomer peak (IIa) can easily be distinguished from the broad cluster background (IIb). For the remaining two regions, only the weighted average β of monomers and clusters can be given. Values for the angular distribution parameter are given in the bottom panel of the figure, and in Table II.

We start our interpretation of Tab. II by inspecting the β values for the HOMO level (region I). This $1b_1$-derived orbital in clusters is involved in hydrogen bonding, as found from calculations,[6,7] and also reflected in the change of binding energy. It can be spectroscopically separated from the monomer photoelectron spectrum. Kinetic energies of the photoelectron lines are approx. 28.5±1 and 48.5±1 eV at the two photon energies. Photoemission from the cluster $1b_1$ level is much more isotropic than from its molecular counterpart. Here we also

note that the molecular $1b_1$ β parameter determined from isolating the molecular lines above the cluster background, agrees excellently with our gas phase reference data. This supports our normalization procedure.

Along the same lines, also the combined $3a_1$ and $1b_2$ β parameters are smaller in magnitude than their molecular counterparts.

The information on size-dependent effects from our data is limited, as the error bars of the second 60 eV data set are too large. (This is because of the low degree of condensation and target pressure fluctuations. We note however that the molecular β for the $1b_1$ region (IIa) agrees with the first data set and the reference measurement.) As a tendency, emission from all other parts of the spectrum is found to be more anisotropic for smaller clusters, which seems plausible in view of what has been said above. Again however, including error bars the values still overlap which impairs us from drawing more definite conclusions.

Thus far, our results are in qualititative agreement with results from studies on noble gas clusters.[12–17]

IV. Discussion

We would now like to discuss possible reasons for the observed reduction in β. Conceivable causes are:

1. changes in the intrinsic β parameter due to modifications of the initial state orbitals, e.g. by hydrogen bonding,

2. intracluster electron scattering,

3. intercluster electron scattering.

A quick estimate shows that, for sample densities that can be produced by our jet, intracluster scattering is much more probable than intercluster scattering (the estimated probability is in the range around 10^{-5}). Therefore, we neglect the latter. In order to assess whether the changes in β can be explained by assuming intracluster scattering, we have estimated the influence of this effect on the PAD by a simple model.

We assume that results from electron scattering experiments on free molecules are applicable to our system. Then, for electron kinetic energies below 100 eV, elastic scattering is by far the most probable outcome of a scattering event.[32] In other words, if intracluster scattering were to play a role, it would lead to the observation of a photoelectron spectrum with a mostly undistorted energy distribution curve, but a PAD that is influenced by scattering.

In order to assess this effect more quantitatively, we have modeled the angular distribution of a photoelectron line with a given β, which undergoes a single elastic scattering event on its way out of the cluster. In a second step, we have obtained an estimate for the probability of such scattering events, and thus for the combined PAD.

We use $p(\theta,\phi)$ for the unscattered electron angular distribution (eq. (1)) and $f(E;\theta,\phi) = f_E(\theta)$ for the differential scattering cross section, which depends on kinetic energy E but not on the azimuthal angle. For the kinetic energies in question, $f_E(\theta)$ has been measured by Cho *et al.*[33] Abbreviating the direction of the detector (θ,ϕ) as $\hat{\mathbf{r}}$, the observed PAD can be written as the convolution of the original photoelectron angular distribution $p(\hat{\mathbf{r}}')$ with the scattering function directional characteristics f_E. Here, f_E depends on the relative angle between $\hat{\mathbf{r}},\hat{\mathbf{r}}'$. We have

$$f_E \otimes p(\hat{\mathbf{r}}) = \int d\hat{\mathbf{r}}'\; p(\hat{\mathbf{r}}')\, f_E(\arccos(\hat{\mathbf{r}}\cdot\hat{\mathbf{r}}')) = \iint d\theta' \sin\theta'\, d\phi'\; p(\theta')\, f_E(\arccos(\hat{\mathbf{r}}\cdot\hat{\mathbf{r}}')). \quad (2)$$

The relative angle $\angle(\hat{\mathbf{r}}, \hat{\mathbf{r}}')$ depends on ϕ', therefore the integration over ϕ' is not trivial. The factor $\sin\theta$ results from the surface element in spherical coordinates. We have evaluated $f_E \otimes p$ by solving the double integral (2) numerically, based on a look-up table filled with the result of Ref. [33].

The parametrization of the angular distribution function is universal for electric dipole processes.[34] The secondary scattering process does not refer to any fixed direction in space. It therefore cannot lead to a change of the general functional relationship of the PAD, but only to a change of the observed value of the β parameter. Calling the angular distribution parameter of an electron ensemble after single scattering β_f, we arrive at $\beta_f = 0.91$ for $\beta = 1.4$, and $\beta_f = 0.45$ for $\beta = 0.7$ at $E = 48$ eV. For $E = 20$ eV, we have $\beta_f = 0.6$ and 0.3, resp. These two cases approximately bridge the interval of kinetic energies in question.

In an experiment, the unscattered part of the electron cloud is observed with its original β, while another part, scattered inside the cluster, is observed with β_f. To obtain an estimate for the probability of single scattering, a structural model of the clusters is needed. Multiple scattering has been neglected, as it is not very probable because of the small cluster size in our experiment.

In search for a simple structural model of our clusters we have studied simulated water cluster geometries. These indicate that water clusters often repeat hexagonal motifs in their arrangement, and are generally quite different from the icosahedral arrangements of rare gas clusters. We have therefore pictured an $N = 80$ water cluster as a cuboid of 4*4*5 water molecules, with an O-O distance of 3 Å.

We model the transmission of electrons through an absorbing continuum of 9*9*12 Å side length. Electrons may start randomly at any position within the cluster, and travel some

distance *l* through the continuum until reaching the surface of the cluster. For the fraction of electrons scattered, we have $q = 1 - \exp(-n\sigma l)$. Using integral cross sections interpolated from Ref. [33] and the density of low density amorphous ice, which we think is appropriate for these small clusters, we have determined first *l* and then *q* for every starting point and every emission direction. We have further integrated over all emission directions, and averaged over all starting points within the cube. Integrals were performed numerically. We then calculated $\beta_{cl}(\text{mod}) = q\beta_f + (1-q)\beta$, where β refers to the monomer measurements given in Table I. Results are given in Table III.

In order to compare the model data for β_{cl} with our experiment, we tried to remove the influence of the overlapping monomer lines from our data. For that we considered the measured β values for the $3a_1$ and $1b_2$ regions as an average of a molecular and a cluster fraction. For a known degree of condensation *c* (defined as the number density of condensed water molecules divided by the total number density), the experimental cluster β_{cl}(exp) can be determined.

The degree of condensation *c* was calculated from the intensity of the $1b_1$ features, with the $1b_1$ cluster area taken from the region I plus 0.5*(region IIb), and the $1b_1$ monomer area from region IIa. Implicit to this analysis, we assume that the ionization cross section for the respective orbital in clusters is equal to the one of monomers. *c* was found to be 0.63 for both the 40 eV and the first 60 eV data set. In the second 60 eV data set, *c* was much lower, and a further analysis of those data was discarded. For the former two data sets, β_{cl}(exp) for the $3a_1$ and $1b_2$ orbitals was calculated using the monomer reference data from our work. Results of this analysis are also in Table III. Error bars have been calculated by propagation of all relevant factors, including a 15 % uncertainty in the assumption of equal partial cross

section between monomer and cluster. For the $1b_1$ orbital, the result measured for region I is repeated, as this part of the spectrum is free from congestion with monomers.

In five of six cases, the β values we measured are lower than the ones derived from the scattering model. While for the 40 eV data, the difference is still within the experimental error bar, for two of the three 60 eV data points the measured data differ by more than one standard deviation. Can this be caused by shortcomings of our model? Indeed, inclusion of multiple scattering might lower the modeled β values further, but this would be a stronger effect at 40 than at 60 eV, as the scattering cross section is larger at the lower energy. However, the agreement with the experiment is worse for the higher energy. Inclusion of inelastic scattering in our model would first of all lead to a preferential loss of bulk signal. This can be assumed to be more isotropic than emission from surface sites. The modeled values would therefore change towards larger β by inelastic scattering.

In order to assess the influence of our assumptions about the scattering cross section on the modeled results, we have arbitrarily increased/decreased the total elastic scattering cross section (the integrated $f(E;\theta,\phi)$) by ±16 %. The resulting changes in the modeled parameter β_{cl} are given as uncertainties in Table III. The model results turn out to be rather robust towards such changes of this input parameter. We note that within our model, the effects would be very similar for a change of cluster size by the same amount. The effect of a change in the cluster shape, from cubic to spherical, would lead to a slight increase of scattering (lower β), but β would also stay within the given uncertainty.

Therefore, we cautiously interpret the results of this study as a first evidence for an intrinsic difference between molecular and cluster PADs, that is one which is not caused by final state electron scattering. Its occurrence in a system like water, where the two least strongly bound molecule orbitals are significantly modified by hydrogen bonding, seems

plausible to the authors. The $1b_1$ orbital, for example, in clusters is calculated as a linear combination of O 2*p*-like lobes, pointing in different directions however.[6,7] If the PAD is composed of the coherent superposition of several such emitting lobes, it is understandable that its β parameter is much lower than in the case of a single emitting lobe. In that respect, our study differs from earlier work on the rare gas clusters, in which the interaction of the electronic charge cloud of different cluster constituents is only via much weaker dispersion forces.[12–17] More detailed experimental investigations of this point are certainly suggested.

V. Conclusions

In the present work, the PADs of water clusters have been experimentally deduced with linearly polarized synchrotron radiation, by rotation of the polarization axis, both at 60 eV and 40 eV. Less anisotropic PADs have been observed for the water clusters than for monomers. Angular distribution values for smaller clusters have a trend towards more anisotropic values.

Intracluster elastic electron scattering is an obvious driving factor for the observed change of the PAD. A scattering model, using molecular electron scattering data[33] as input, has been used to quantitatively explain the decrease of PAD β parameters. Values calculated for β however are consistently slightly larger than the measured ones, which points to the possibility of additional β changes due to initial state effects.

Our results clearly show that angular distribution effects have to be taken into account when photoelectron spectra from a liquid jet are measured outside of the magic angle, and that molecular measurements cannot represent these effects in the condensed phase in a quantitative manner. While this work was finalized, a discussion of angular distribution effects in photoemission from liquid water came to our attention.[35]

Acknowledgements

UH would like to thank Stephan Thürmer and Bernd Winter for making their results available prior to publication, and for useful discussion. The support of W. Frentrup and A. Gaupp for using the angle changing undulator is gratefully acknowledged. The work presented here has been also supported by the Swedish Research Council (VR). This work was supported by the Deutsche Forschungsgemeinschaft (HE 3060/5-1). We thank HZB for the allocation of synchrotron radiation beamtime (project No. 2010_1_91186).

TABLE I. Angular distribution parameter β for the outer valence orbitals of gas phase water molecules. Data from Ref. [2] have been interpolated to the photon energies of our study.

Orbital	Photon energy	β (this work)	β (Ref. [2])
$1b_1$	40 eV	1.38(8)	1.42(5)
$3a_1$		1.08(8)	1.15(4)
$1b_2$		0.75(12)	0.74(3)
$1b_1$	60 eV	1.59(8)	1.53(4)
$3a_1$		1.41(8)	1.35(4)
$1b_2$		1.04(12)	1.00(2)

TABLE II. Angular distribution parameter β for the outer valence orbitals of a molecular jet containing a mixture of water molecules and water clusters. See text for details.

Region	Assignment	β
Photon energy 40 eV, $\langle N \rangle$ = 58(5)		
I	$1b_1$ (cluster)	0.79(10)
II	$1b_1$ (mol.), $1b_1$ (cl.), $3a_1$ (cl.)	1.21(6)
IIa	$1b_1$ (mol.)	1.46(8)
IIb	$1b_1$ (cl.), $3a_1$ (cl.)	0.83(12)
III	$3a_1$ (mol.), $3a_1$ (cl.)	0.86(10)
IV	$1b_2$ (mol.), $1b_2$ (cl.)	0.54(10)
Photon energy 60 eV, $\langle N \rangle$ > 84, set 1, Cluster/Total=63%		
I	$1b_1$ (cluster)	1.17(6)
II	$1b_1$ (mol.), $1b_1$ (cl.), $3a_1$ (cl.)	1.36(6)
IIa	$1b_1$ (mol.)	1.62(8)
IIb	$1b_1$ (cl.), $3a_1$ (cl.)	1.08(8)
III	$3a_1$ (mol.), $3a_1$ (cl.)	1.14(6)
IV	$1b_2$ (mol.), $1b_2$ (cl.)	0.82(10)
Photon energy 60 eV, $\langle N \rangle$ = 84, set 2, Cluster/Total=28%		
I	$1b_1$ (cluster)	1.27(8)
II	$1b_1$ (mol.), $1b_1$ (cl.), $3a_1$ (cl.)	1.54(8)
IIa	$1b_1$ (mol.)	1.60(10)
IIb	$1b_1$ (cl.), $3a_1$ (cl.)	1.11(10)
III	$3a_1$ (mol.), $3a_1$ (cl.)	1.22(8)
IV	$1b_2$ (mol.), $1b_2$ (cl.)	0.85(12)

TABLE III. Angular distribution parameter β for the outer valence orbitals of water clusters. β_{cl}(exp): measured, gas phase contribution removed (this work). β_{cl} (model): single scattering model (this work). β(mol.): molecular β parameter, repeated from Table I for convenience. Error given for β_{cl} (model) refers to the change of calculated β parameter upon 16 % change of the elastic scattering cross section, used as an input. See text for details.

Orbital	Photon energy	β_{cl}(exp)	β_{cl}(model)	β(mol.)
$1b_1$	40 eV	0.83(8)	0.91(4)	1.38(8)
$3a_1$		0.73(16)	0.70(3)	1.08(8)
$1b_2$		0.42(16)	0.49(2)	0.75(12)
$1b_1$	60 eV	1.17(8)	1.31(3)	1.59(8)
$3a_1$		0.99(12)	1.15(3)	1.41(8)
$1b_2$		0.70(18)	0.85(2)	1.04(12)

FIG. 1. The partition for fitting of the spectrum that contains both the cluster and monomer signals. The area I corresponds to the $1b_1$ cluster, IIa is for the pure molecule $1b_1$, the bottom IIb area is attributed half to $1b_1$ cluster and the rest to $3a_1$ cluster, the area III is for $3a_1$ both cluster and monomer, and the area IV is for $1b_2$ cluster and monomer.

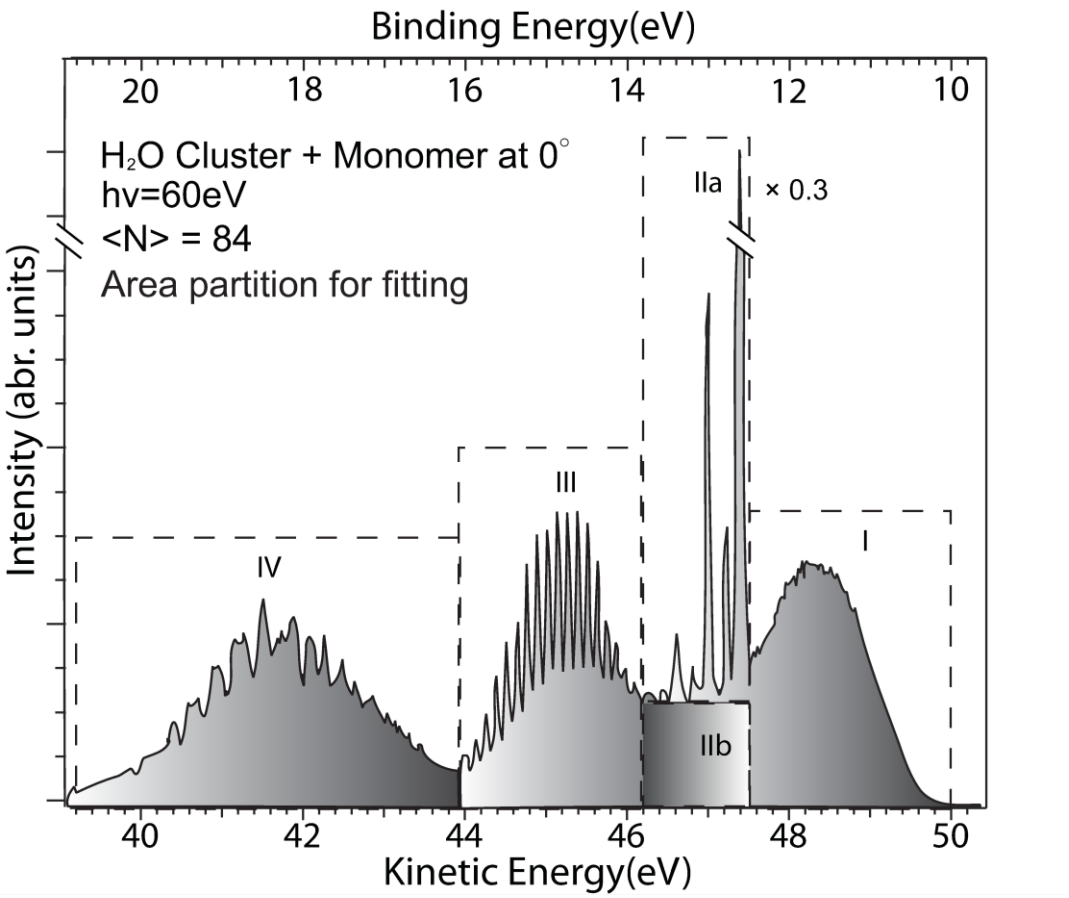

FIG. 2. Top panel: Photoelectron spectrum of a mixture of water clusters with monomers, recorded at a photon energy of 60 eV at an angle θ of 0° and at the 'magic angle' of 54.7° (dotted and solid trace). Bottom panel: The β parameter for different orbitals, as given in Table II.

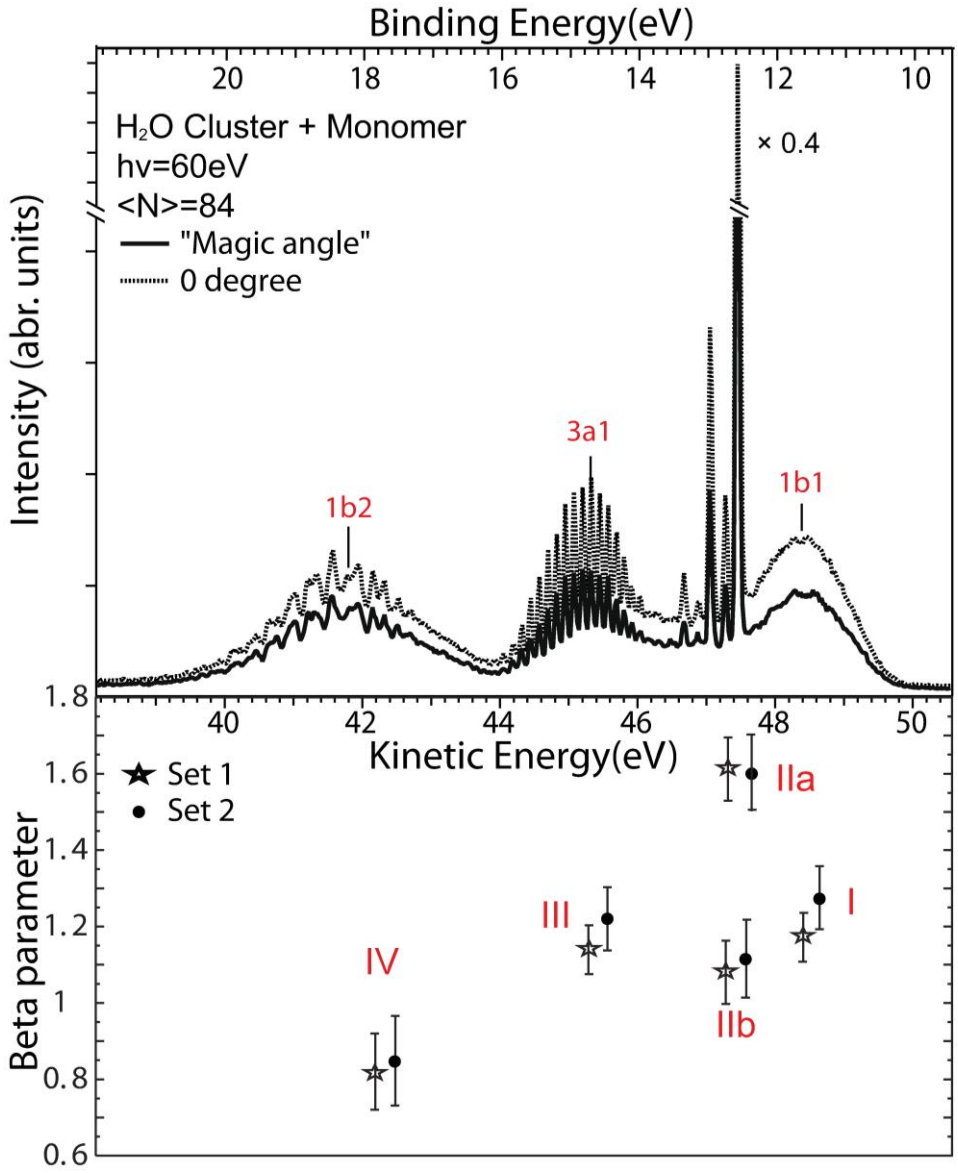

REFERENCES

[1] L. Karlsson, L. Mattson, R. Jadrny, R.G. Albridge, S. Pinchas, T. Bergmark, and K. Siegbahn, The Journal of Chemical Physics **62**, 4745 (1975).

[2] M.S. Banna, B.H. McQuaide, R. Malutzki, and V. Schmidt, The Journal of Chemical Physics **84**, 4739 (1986).

[3] B. Winter, R. Weber, W. Widdra, M. Dittmar, M. Faubel, and I. V. Hertel, The Journal of Physical Chemistry A **108**, 2625 (2004).

[4] D. Nordlund, M. Odelius, H. Bluhm, H. Ogasawara, L.G.M. Pettersson, and a. Nilsson, Chemical Physics Letters **460**, 86 (2008).

[5] O. Björneholm, F. Federmann, S. Kakar, and T. Möller, The Journal of Chemical Physics **111**, 546 (1999).

[6] S. Barth, M. Oncák, V. Ulrich, M. Mucke, T. Lischke, P. Slavícek, and U. Hergenhahn, The Journal of Physical Chemistry. A **113**, 13519 (2009).

[7] P. Cabral do Couto, S.G. Estácio, and B.J. Costa Cabral, The Journal of Chemical Physics **123**, 54510 (2005).

[8] B. Brena, D. Nordlund, M. Odelius, H. Ogasawara, A. Nilsson, and L.G.M. Pettersson, Physical Review Letters **93**, 148302 (2004).

[9] U. Becker and D.A. Shirley, in *VUV- and Soft X-Ray Photoionization*, edited by U. Becker and D.A. Shirley (Plenum Press, New York, 1996), pp. 13–180.

[10] C.C. Pradzynski, R.M. Forck, T. Zeuch, P. Slavíček, and U. Buck, Science **337**, 1529 (2012).

[11] C.M. Truesdale, S. Southworth, P.H. Kobrin, D.W. Lindle, G. Thornton, and D.A. Shirley, The Journal of Chemical Physics **76**, 860 (1982).

[12] G. Öhrwall, M. Tchaplyguine, M. Gisselbrecht, M. Lundwall, R. Feifel, T. Rander, J. Schulz, R.R.T. Marinho, a Lindgren, S.L. Sorensen, S. Svensson, and O. Björneholm, Journal of Physics B: Atomic, Molecular and Optical Physics **36**, 3937 (2003).

[13] D. Rolles, H. Zhang, Z.D. Pesic, R.C. Bilodeau, A. Wills, E. Kukk, B.S. Rude, G.D. Ackerman, J.D. Bozek, R. Díez Muiño, F.J. García de Abajo, and N. Berrah, Physical Review A **75**, 31201 (2007).

[14] D. Rolles, Z.D. Pesic, H. Zhang, R.C. Bilodeau, J.D. Bozek, and N. Berrah, Journal of Physics: Conference Series **88**, 012003 (2007).

[15] H. Zhang, D. Rolles, Z.D. Pešić, J.D. Bozek, and N. Berrah, Physical Review A **78**, 063201 (2008).

[16] D. Rolles, H. Zhang, Z. D. Pesic, J. D. Bozek, and N. Berrah, Chemical Physics Letters **468**, 148 (2009).

[17] H. Zhang, D. Rolles, J.D. Bozek, and N. Berrah, Journal of Physics B: Atomic, Molecular and Optical Physics **42**, 105103 (2009).

[18] M. Förstel, M. Mucke, T. Arion, T. Lischke, S. Barth, V. Ulrich, G. Öhrwall, O. Björneholm, U. Hergenhahn, and A. M. Bradshaw, Physical Review B **82**, 125450 (2010).

[19] A. Zecca, G.P. Karwasz, and R.S. Brusa, Rivista Del Nuovo Cimento **19**, 1 (1996).

[20] S. Barth, Ph.D. thesis, Technical University Berlin, 2007 (http://opus.kobv.de/tuberlin/volltexte/2007/1581/).

[21] S. Sasaki, Nuclear Instruments and Methods in Physics Research Section A: Accelerators, Spectrometers, Detectors and Associated Equipment **347**, 83 (1994).

[22] J. Bahrdt, W. Frentrup, A. Gaupp, M. Scheer, W. Gudat, G. Ingold, and S. Sasaki, Nuclear Instruments and Methods in Physics Research Section A: Accelerators, Spectrometers, Detectors and Associated Equipment **467-468**, 21 (2001).

[23] K. Godehusen, H.-C. Mertins, T. Richter, P. Zimmermann, and M. Martins, Physical Review A **68**, 012711 (2003).

[24] H. Derenbach and V. Schmidt, Journal of Physics B **17**, 83 (1984).

[25] J. Bahrdt, R. Follath, W. Frentrup, A. Gaupp, M. Scheer, Proceedings of the SRI 2009: The 10th International Conference on Synchrotron Radiation Instrumentation, Melbourne, Australia, 2009, edited by R. Garrett, I. Gentle, K. Nugent, S. Wilkins (AIP Conference Proceedings), Vol. **1234**, p. 335 (2010).

[26] C. Steinbach, P. Andersson, J.K. Kazimirski, U. Buck, V. Buch, and T.A. Beu, Journal of Physical Chemistry A **108**, 6165 (2004).

[27] C. Bobbert, S. Schütte, C. Steinbach, and U. Buck, The European Physical Journal D **19**, 183 (2002).

[28] See Supplementary Material for a a documentation of the expansion conditions and reference photoelectron spectra of molecular water.

[29] J.-H. Guo, Y. Luo, A. Augustsson, J.-E. Rubensson, C. Såthe, H. Ågren, H. Siegbahn, and J. Nordgren, Physical Review Letters **89**, 137402 (2002).

[30] M. V Vega, C. Lavín, and A.M. Velasco, The Journal of Chemical Physics **136**, 214308 (2012).

[31] G. Öhrwall, R.F. Fink, M. Tchaplyguine, L. Ojamäe, M. Lundwall, R.R.T. Marinho, a Naves de Brito, S.L. Sorensen, M. Gisselbrecht, R. Feifel, T. Rander, A. Lindblad, J. Schulz, L.J. Saethre, N. Mårtensson, S. Svensson, and O. Björneholm, The Journal of Chemical Physics **123**, 054310 (2005).

[32] Y. Itikawa and N. Mason, Journal of Physical and Chemical Reference Data **34**, 1 (2005).

[33] H. Cho, Y.S. Park, H. Tanaka, and S.J. Buckman, Journal of Physics B: Atomic, Molecular and Optical Physics **37**, 625 (2004).

[34] A. Bechler and R.H. Pratt, Physical Review A **42**, 6400 (1990).

[35] S. Thürmer, R. Seidel, M. Faubel, W. Eberhardt, J.C. Hemminger, S.E. Bradforth, and B. Winter, to be published.

SUPPLEMENTARY MATERIAL

Expansion parameters and determination of cluster size

The detailed expansion parameters which were used for cluster production are given in Table IV. All experiments used a nozzle of d = 80 µm diameter and α = 15° half opening angle. The stagnation pressure p was derived as the vapour pressure of water at the reservoir temperature given. Scaling laws state a relation between the parameters of a supersonic expansion used for cluster production and the mean cluster size produced in it. Although thermodynamically inspired essentially they are empirical. The one used in our work is due to Bobbert *et al.* [27]. It reads:

$$\langle N \rangle = D \left(p\, d_{eq}^{\,q} \left(\frac{T_n}{T_c r_c} \right)^{q-3} \frac{1}{1000\, k T_n} \right)^a ,$$

where a, q and D are empirical parameters which for water clusters were optimized to values of 1.886, 0.634 and 11.6. T_c = 5684 K and r_c = 3.19 Å are the characteristic temperature and characteristic radius for water, see Ref. 27. $d_{eq} := 0.933\, d / \tan\alpha$ is the 'equivalent diameter', k the Boltzmann constant. Within the given formalism, cluster sizes have a systematic uncertainty of approx. 7 % from an inaccuracy of the thermocouple reference temperature, which influences the temperature measurement. For the 40 eV data set, a thermocouple reading of the nozzle temperature was not available, and T_n was estimated from the power consumption of the nozzle heater. In the first 60 eV data set, He seeding gas was used. As this fosters aggregation of the water molecules, we give the scaling law result for the mean cluster size as a lower limit. In the second 60 eV data set, no seeding gas was used.

TABLE IV. Expansion parameters used for production of water clusters: T_r : Reservoir temperature, p : stagnation pressure, T_n : Nozzle temperature, $\langle N \rangle$: Cluster mean size as given by Ref. 27.

	T_r (° C)	p (mbar)	T_n (° C)	$\langle N \rangle$
40eV	102.5	1106	105-117	52-63
60eV set 1	110	1432	117	>84
60eV set 2	110	1432	117	84

Photoelectron angular distribution of water monomers

The photoelectron spectrum of water monomers has been presented a number of times (see e.g. Ref.s 1, 2). For comparison, we here present two of the reference spectra recorded for this work:

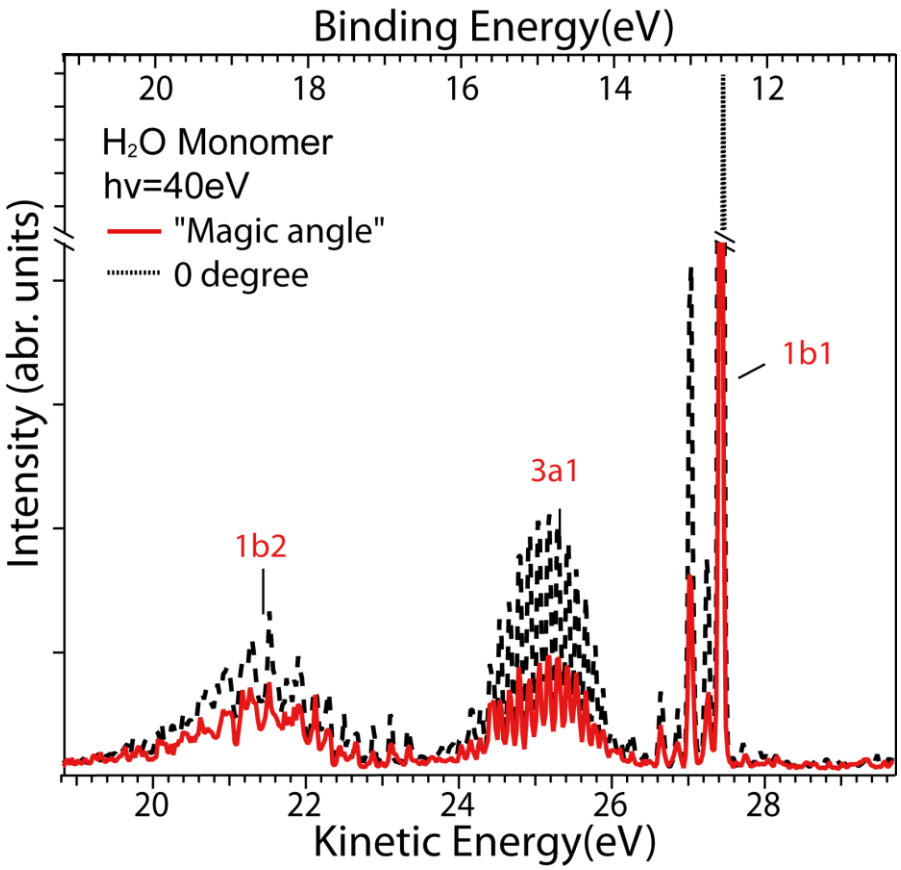

FIG. 3. Photoelectron spectrum water monomer, recorded at a photon energy of 40 eV at an angle θ of 0° and at the 'magic angle' of 54.7° (dotted and solid trace).